ChemComm

COMMUNICATION

View Article Online
View Journal | View Issue

Cite this: *Chem. Commun.*, 2015, 51, 13500

Received 14th May 2015,
Accepted 13th July 2015

DOI: 10.1039/c5cc04022a

www.rsc.org/chemcomm

FeV_2S_4 as a high capacity electrode material for sodium-ion batteries†

Markus Krengel,[a] Philipp Adelhelm,[b] Franziska Klein[c] and Wolfgang Bensch*[a]

Iron vanadium sulfide (FeV_2S_4) was synthesized *via* a high temperature solid state reaction and was investigated as a cheap anode material for Na and Li ion batteries. Discharge capacities as high as 723 mA h g^{-1} (Na) and 890 mA h g^{-1} (Li) were found for half-cell measurements at room temperature. The capacity of the Na–FeV_2S_4 system remained constant at 529 mA h g^{-1} after the 10th cycle with an area capacity of 2.7 mA h cm^{-2} being very close to that of conventional Li-ion technology.

Since the price of fossil fuels has increased dramatically in the last few decades and the world-wide energy demand is still rising, the generation and storage of environmentally friendly and renewable energy has become a key issue for modern society.[1–3] In the past the focus on energy storage devices was on lithium ion batteries (LIB) due to their beneficial properties *e.g.* high power densities, fast reaction kinetics, high voltage *etc.* For large scale energy storage enormous amounts of Li would be required. Despite the fact that Li is a widely distributed element on Earth, it cannot be regarded as an abundant element.[4] An alternative and the most promising element replacing Li is Na, considering the standard potential, atomic weight, the low price and especially the nearly unlimited availability.[5,6] Reports about suitable Na cathode materials were published during the last few years covering a variety of mainly oxidic compounds.[7–14] Graphite was considered to be a non-suitable anode material because Na barely reacts to form staged intercalation compounds, which is assumed to be the consequence of an unfavourable disproportion between the graphite structure and the size of the Na^+ ion.[15] Recent studies show that this disproportion can be overcome by the use of co-intercalation phenomena using solvent molecules to form ternary graphite intercalation compounds with capacities close to 100 mA h g^{-1}.[16] Besides graphite, the performance of other carbon based anode materials has gradually improved during the last few years, but overall, issues such as power capability and irreversible capacity loss remain. Further, potential anode materials are much less explored and are mostly based on main group elements, alloys, phosphides and a variety of oxidic compounds as was recently reviewed in ref. 17. In most cases the reaction between Na and the anode material leads to high capacities during conversion reactions, which can be regarded as a promising route. While conversion reactions with Li were studied already a long time ago[18–20] and are still being investigated intensively,[21–24] the literature on conversion reactions of sulphide compounds applying Na is limited and only a few sulphides were studied.[25–27] A focus of research lies on layered dichalcogenide compounds such as SnS_2,[28] MoS_2,[29–35] NbS_2,[36] WS_2,[34] or TiS_2.[37] But main group sulfides like Sb_2S_3 were also studied concerning the electrochemical behavior in Na batteries.[38] For binary compounds conversion reactions can be generally formulated according to eqn (1):

$$M_xQ_y + 2y\ e^- + 2y\ Na^+ \leftrightarrow x[M]^{\pm 0} + y\ Na_wQ_v \qquad (1)$$

(M = metal, Q = O, S, Se).

A recently published paper dealing with binary transition metal (TM) compounds for conversion reactions showed that the difference in cell potentials between conversion reactions of binary sulfides with Na and Li amounts to +0.39 V assuming the formation of A_2S as reaction products (A = Li, Na). Obviously, such a conversion of a simple compound offers attractive capacities for energy storage.[39] However, conversion reactions also have disadvantages like *e.g.* high volume expansion, which can reduce the cycle stability drastically. The most challenging intrinsic limitation of conversion reactions is the use or the formation of poorly conducting compounds such as Li_2S or Na_2S. Although the formation of insulating compounds is

[a] *Christian-Albrechts-Universität zu Kiel, Institute of Inorganic Chemistry, Max-Eyth-Straße 2, 24118 Kiel, Germany. E-mail: wbensch@ac.uni-kiel.de; Fax: +49-481-880-1520*
[b] *Friedrich-Schiller-University Jena, Institute for Technical Chemistry and Environmental Chemistry, Center for Energy and Environmental Chemistry (CEEC), Lessingstraße 12, 07743 Jena, Germany*
[c] *Justus-Liebig-Universität Giessen, Institut für Physikalische Chemie, Heinrich-Buff-Ring 58, 35392 Giessen, Germany*

† Electronic supplementary information (ESI) available. See DOI: 10.1039/c5cc04022a

highly undesired, the electrodes usually still remain fairly active, as the first Li or Na insertion leads to the formation of a complex, nanoscopic structure. Nevertheless, as a result of the phase separation, high overpotentials and poor reversibility are typical for most conversion reactions. A large amount of conducting additive, typically around 15–30 wt%, is therefore commonly added in order to achieve a reasonable performance. Conversion reactions requiring small amounts of conductive additive are therefore highly desirable. Assuming the electrode reaction proceeds ideally as formulated in eqn (1), defined voltage plateaus would be expected during cycling. However, sloping potentials are observed during cycling once the nanoscopic structure has formed during the first insertion process. The more phases that form during the first insertion, the more finely divided the nanostructure that might evolve, so using ternary instead of binary compounds as the starting material might enable a better reversibility while showing similar voltage profiles. Moreover, sodium based conversion reaction with sulfides might lead to several additional intermediate phases such as Na_2S, Na_2S_2, Na_2S_4 or Na_2S_5.

On the basis of the considerations presented in ref. 39 and above, we investigated FeV_2S_4 (see the ESI† for Experimental details), which contains several potential electro-chemical redox-active elements. The compound FeV_2S_4 has been intensively studied concerning its magnetic and structural properties but not as an anode material in sodium or lithium ion batteries so far. FeV_2S_4 crystallizes in the monoclinic space group $I2/m$ in the V_3S_4 structure, which is a distorted NiAs-type structure with the Fe cations preferably occupying the metal deficient layers (inset Fig. 1) and shows metallic conductivity with a resistivity of 1.2×10^{-3} Ω cm.[40–49]

The Rietveld refinement of the X-ray powder data reveals a phase pure material (Fig. 1). The lattice parameters were determined as a = 5.853(3) Å, b = 3.291(9) Å, c = 11.257(9) Å and β = 91.92(1)°, similar to the data reported.[45,48] The elemental analysis performed with EDX yields a composition close to a stoichiometric material (EDX: $FeV_2S_{4.1}$). In SEM images needle and plate like crystals with a broad size distribution are seen (Fig. S1, ESI†). The phase diagram of Na and S shows numerous sulfides as mentioned above, so several reactions can be assumed during Na uptake by the host material.[27,50]

$$8Na + FeV_2S_4 \rightarrow Fe + 2V + 4Na_2S \quad (2)$$

$$4Na + FeV_2S_4 \rightarrow Fe + 2V + 2Na_2S_2 \quad (3)$$

$$4Na + 2FeV_2S_4 \rightarrow 2Fe + 4V + 2Na_2S_4 \quad (4)$$

$$8Na + 5FeV_2S_4 \rightarrow 5Fe + 10V + 4Na_2S_5 \quad (5)$$

In contrast, the Li–S phase diagram shows only Li_2S, equal to eqn (2), under ambient conditions. The theoretical capacity according to eqn (2)–(5) is 750, 375, 188 and 150 mA h g^{-1}, respectively. Fig. 2 displays the voltage profiles of sodium and lithium insertion/deinsertion into FeV_2S_4 at a constant current rate of 75 mA g^{-1} between 0 and 3 V. The Na–FeV_2S_4 cell shows a sudden potential drop at the beginning of discharge followed by a long plateau at 0.3 V and finally a steady drop to 0 V. The initial discharge capacity of 723 mA h g^{-1} is close to the theoretical value calculated on the basis of the reaction presented in eqn (2), *i.e.* it seems that 7.7 Na can be inserted into the host material. However, it is clear that the well-known solid electrolyte interphase (SEI) formation also partially contributes to the capacity. An exact verification of the proposed reaction

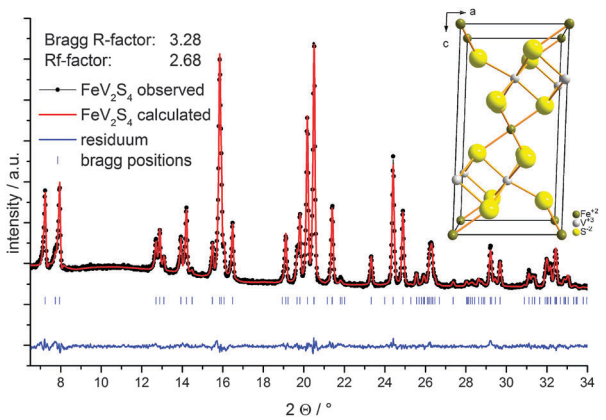

Fig. 1 Rietveld refinement of XRD pattern of FeV_2S_4 and unit cell (inset). Final observed (dots), calculated (red) and difference (blue) profiles. Reflection positions are marked as vertical bars.

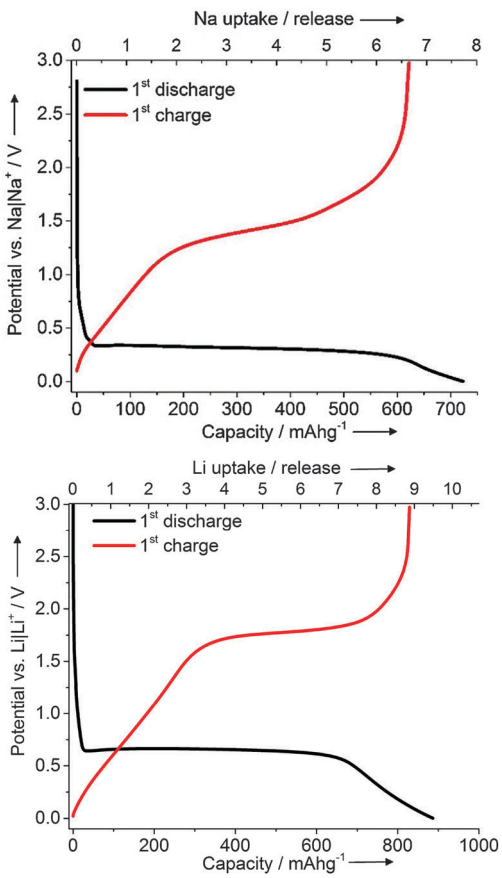

Fig. 2 The first charge/discharge curve of FeV_2S_4 *vs.* Na (top) and Li (bottom).

equations based on the achieved capacity is therefore not possible.

The first charge curve shows a constant increase of the potential up to 1.3 V followed by a plateau region between 1.3 and 1.6 V. Charging ends with a sudden potential increase. At about 3 V a charge capacity of 622 mA h g^{-1} is reached corresponding to the extraction of 6.6 Na per formula unit. We note that the fraction of active material is 80 wt% and hence comparably high for conversion electrodes. Only 10 wt% of conductive additive has been added during electrode preparation. With an active mass loading of around 3 mg cm^{-2}, the observed values correspond to an area capacity of around 2.7 mA h cm^{-2} which is comparable to conventional Li-ion technology. On the other hand, we observed that a long cycle life so far is limited by side reactions with the electrolyte. Future studies therefore also need to be directed towards identification of suitable electrolytes.

The Li–FeV_2S_4 cell exhibits a very similar profile, with a long plateau at 0.66 V during discharge followed by a drop to 0 V at the end of the reaction. For the charge curve a steady increase of the voltage is observed with a plateau located in the region of 1.7–1.9 V. The discharge and charge capacities are 890 and 830 mA h g^{-1} respectively, which are higher than the theoretically expected capacity of 750 mA h g^{-1} assuming a full conversion of Fe^{2+} and V^{3+} to the metals and the formation of Li_2S (eqn (2)). The phenomenon of additional capacity in Li conversion reactions is well documented in the literature and additional capacitive charge storage at interfaces[51,52] and/or electrolyte decomposition[53–57] are often invoked to explain this observation.

In Fig. 3 the evolution of the discharge/charge curves during cycling are displayed. The second discharge traces differ from the first curve for both systems. The long plateau region at 0.3 V (Na) respectively 0.66 V (Li) disappeared and a slope occurred for both Na– and Li–FeV_2S_4 cells.

In the Na–FeV_2S_4 cell the capacity of the second discharge decreased to 596 mA h g^{-1} which is 82% of the initial capacity and then stabilized at 529 mA h g^{-1} after the 10th cycle (73% of the initial capacity, cycling of 5.6 Na) reaching a Coulomb efficiency of 99%. This behavior differs from that of the Li–FeV_2S_4 cell. For this cell the capacity loss in the second cycle is less pronounced giving a capacity of 853 mA h g^{-1} (96% of initial capacity) but showing a continuous capacity fade after every cycle with a remaining capacity of only 400 mA h g^{-1} after the 15th cycle (45% of the initial capacity).

Although reversible charge storage is found, the voltage profiles and complementary cyclic voltammetry measurements (Fig. S2, ESI†) are not suited to formulate the detailed reaction mechanisms, which is a common challenge for conversion reactions. More insight into the reaction mechanism might be obtained by *in situ* high resolution X-ray diffraction and X-ray absorption spectroscopy measurements (XAS). *Ex situ* XRD measurements reveal a fast conversion of the anode material into an amorphous state upon first discharge. No recrystallization was observed during charging to 3 V (Fig. S3, ESI†).

The sodium storage behavior of FeV_2S_4 at different currents is shown in Fig. 4. Capacities of around 500 to 550 mA h g^{-1} were achieved at currents of 75 mA g^{-1} and 150 mA g^{-1}. Around 350 mA h g^{-1} were found at a current of 375 mA g^{-1}.

Overall, this study demonstrates that electrochemically driven reactions of FeV_2S_4 with Na and Li are at least partially reversible and deliver high capacities, making the material an interesting candidate for primary and/or secondary Li or Na batteries. After an initial activation cycle, the Na–FeV_2S_4 system shows a small capacity fade of 12% within the first 10 cycles when discharged with a constant current of 75 mA g^{-1} (this value corresponds to a C-rate of C/10 assuming full conversion after eqn (2)). The presence of vanadium seems to be beneficial regarding capacity fading and cyclability compared to the Na–FeS_2 system, showing a severe capacity fade within the first

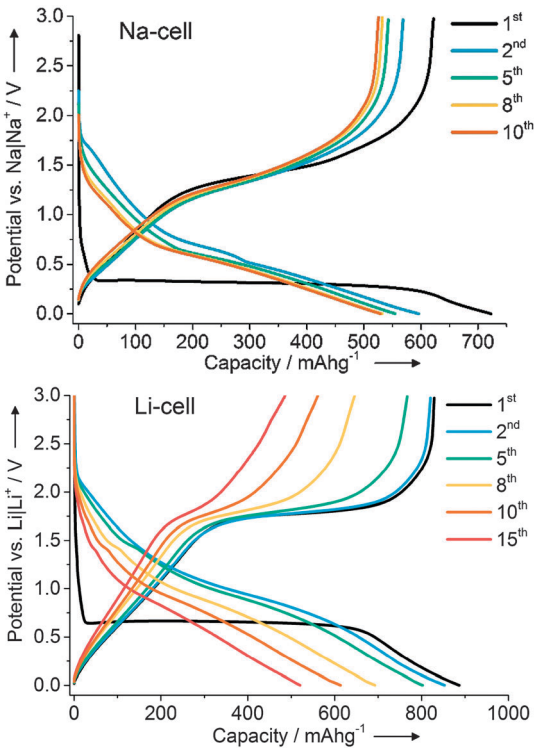

Fig. 3 Change of discharge curves of Na– (top) and Li–FeV_2S_4 cell (bottom).

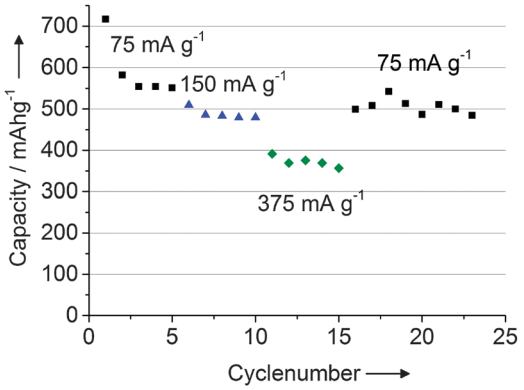

Fig. 4 Cyclic performance of the Na–FeV_2S_4 system at different C rates.

10 cycles of about 55% when fully converted to metallic Fe and sodium sulfide.[27,58] In a recent work, improved cycle stability was achieved by restricting the cut-off voltage to 0.8 V to avoid a full conversion of FeS_2 leading to a constant capacity of 240 mA h g^{-1}.[59]

The extraordinary performance of the Na–FeV_2S_4 cell becomes obvious when comparing the present results with those reported for other sulfides. For a MoS_2–carbon composite a capacity of ≈400 mA h g^{-1} was reported.[34] About 250 mA h g^{-1} were obtained for a MoS_2-graphene material.[35] Even much lower capacities (<200 mA h g^{-1}) were reported for the Na–TiS_2 system[37] and for Na–NbS_2.[36]

A comparable capacity to that obtained for Na–FeV_2S_4 was only achieved for sulfide–carbon composites with high amounts of added carbon black and low loading rates of about 1 mg cm^{-2} while we studied a bare material with 80 wt% active material and reasonable loading rates of 3 mg cm^{-1} on the electrode films.[32,36,60]

In conclusion, the use of ternary sulfides such as FeV_2S_4 might enable the development of electrode materials for new electrochemical storage devices, with particular focus on sodium as the abundant element. In addition, the complete understanding of the reaction mechanism requires suitable *in operando* investigations, which will be performed in the future.

Notes and references

1 J. M. Dargay and D. Gately, *Energy Policy*, 2010, **38**, 6261–6277.
2 N. L. Panwar, S. C. Kaushik and S. Kothari, *Renewable Sustainable Energy Rev.*, 2011, **15**, 1513–1524.
3 A. S. Aricò, P. Bruce, B. Scrosati, J.-M. Tarascon and W. Van Schalkwijk, *Nat. Mater.*, 2005, **4**, 366–377.
4 R. S. Carmichael, *Practical Handbook of Physical Properties of Rocks and Minerals*, CRC Press, Boca Raton, 1989.
5 B. L. Ellis and L. F. Nazar, *Curr. Opin. Solid State Mater. Sci.*, 2012, **16**, 168–177.
6 D. Kundu, E. Talaie, V. Duffort and L. F. Nazar, *Angew. Chem.*, 2015, **127**, 3495–3513.
7 P. Barpanda, G. Liu, C. D. Ling, M. Tamaru, M. Avdeev, S.-C. Chung, Y. Yamada and A. Yamada, *Chem. Mater.*, 2013, **25**, 3480–3487.
8 M. Xu, L. Wang, X. Zhao, J. Song, H. Xie, Y. Lu and J. B. Goodenough, *Phys. Chem. Chem. Phys.*, 2013, **15**, 13032.
9 D. Su, C. Wang, H. Ahn and G. Wang, *Chem. – Eur. J.*, 2013, **19**, 10884–10889.
10 Z. Liu, Y.-Y. Hu, M. T. Dunstan, H. Huo, X. Hao, H. Zou, G. Zhong, Y. Yang and C. P. Grey, *Chem. Mater.*, 2014, **26**, 2513–2521.
11 X. Liu, X. Wang, A. Iyo, H. Yu, D. Li and H. Zhou, *J. Mater. Chem. A*, 2014, **2**, 14822.
12 S. Guo, H. Yu, Z. Jian, P. Liu, Y. Zhu, X. Guo, M. Chen, M. Ishida and H. Zhou, *ChemSusChem*, 2014, **7**, 2115–2119.
13 J. Song, M. Xu, L. Wang and J. B. Goodenough, *Chem. Commun.*, 2013, **49**, 5280.
14 Y.-U. Park, D.-H. Seo, H.-S. Kwon, B. Kim, J. Kim, H. Kim, I. Kim, H.-I. Yoo and K. Kang, *J. Am. Chem. Soc.*, 2013, **135**, 13870–13878.
15 J. Sangster, *J. Phase Equilib. Diffus.*, 2007, **28**, 571–579.
16 B. Jache and P. Adelhelm, *Angew. Chem., Int. Ed.*, 2014, **53**, 10169–10173.
17 Y. Kim, K.-H. Ha, S. M. Oh and K. T. Lee, *Chem. – Eur. J.*, 2014, **20**, 11980–11992.
18 M. M. Thackeray and J. Coetzer, *Mater. Res. Bull.*, 1981, **16**, 591–597.
19 H. Ikeda and S. Narukawa, *J. Power Sources*, 1983, **9**, 329–334.
20 M. Thackeray, S. Baker, K. Adendorff and J. Goodenough, *Solid State Ionics*, 1985, **17**, 175–181.
21 M. Sathiya, K. Ramesha, G. Rousse, D. Foix, D. Gonbeau, A. S. Prakash, M. L. Doublet, K. Hemalatha and J.-M. Tarascon, *Chem. Mater.*, 2013, **25**, 1121–1131.
22 B. C. Melot and J.-M. Tarascon, *Acc. Chem. Res.*, 2013, **46**, 1226–1238.
23 D. Liu, W. Zhu, J. Trottier, C. Gagnon, F. Barray, A. Guerfi, A. Mauger, H. Groult, C. M. Julien, J. B. Goodenough and K. Zaghib, *RSC Adv.*, 2014, **4**, 154.
24 K. Zaghib, A. Mauger, H. Groult, J. Goodenough and C. Julien, *Materials*, 2013, **6**, 1028–1049.
25 J.-S. Kim, H.-J. Ahn, H.-S. Ryu, D.-J. Kim, G.-B. Cho, K.-W. Kim, T.-H. Nam and J. H. Ahn, *J. Power Sources*, 2008, **178**, 852–856.
26 J.-S. Kim, D.-Y. Kim, G.-B. Cho, T.-H. Nam, K.-W. Kim, H.-S. Ryu, J.-H. Ahn and H.-J. Ahn, *J. Power Sources*, 2009, **189**, 864–868.
27 T. B. Kim, J. W. Choi, H. S. Ryu, G. B. Cho, K. W. Kim, J. H. Ahn, K. K. Cho and H. J. Ahn, *J. Power Sources*, 2007, **174**, 1275–1278.
28 B. Qu, C. Ma, G. Ji, C. Xu, J. Xu, Y. S. Meng, T. Wang and J. Y. Lee, *Adv. Mater.*, 2014, **26**, 3854–3859.
29 C. Zhu, X. Mu, P. A. van Aken, Y. Yu and J. Maier, *Angew. Chem.*, 2014, **126**, 2184–2188.
30 M. Mortazavi, C. Wang, J. Deng, V. B. Shenoy and N. V. Medhekar, *J. Power Sources*, 2014, **268**, 279–286.
31 M. Pumera, Z. Sofer and A. Ambrosi, *J. Mater. Chem. A*, 2014, **2**, 8981.
32 W.-H. Ryu, J.-W. Jung, K. Park, S.-J. Kim and I.-D. Kim, *Nanoscale*, 2014, **6**, 10975–10981.
33 J. Park, J.-S. Kim, J.-W. Park, T.-H. Nam, K.-W. Kim, J.-H. Ahn, G. Wang and H.-J. Ahn, *Electrochim. Acta*, 2013, **92**, 427–432.
34 Y.-X. Wang, K. H. Seng, S.-L. Chou, J.-Z. Wang, Z. Guo, D. Wexler, H.-K. Liu and S.-X. Dou, *Chem. Commun.*, 2014, **50**, 10730.
35 L. David, R. Bhandavat and G. Singh, *ACS Nano*, 2014, **8**, 1759–1770.
36 Y. Liao, K.-S. Park, P. Xiao, G. Henkelman, W. Li and J. B. Goodenough, *Chem. Mater.*, 2013, **25**, 1699–1705.
37 H.-S. Ryu, J.-S. Kim, J.-S. Park, J.-W. Park, K.-W. Kim, J.-H. Ahn, T.-H. Nam, G. Wang and H.-J. Ahn, *J. Electrochem. Soc.*, 2013, **160**, A338–A343.
38 D. Y. W. Yu, P. V. Prikhodchenko, C. W. Mason, S. K. Batabyal, J. Gun, S. Sladkevich, A. G. Medvedev and O. Lev, *Nat. Commun.*, 2013, **4**, 2922.
39 F. Klein, B. Jache, A. Bhide and P. Adelhelm, *Phys. Chem. Chem. Phys.*, 2013, **15**, 15876.
40 M. Chevreton and A. Sapet, *Compt. Rend. Acad. Sci. Paris*, 1965, **261**, 928–930.
41 Y. Oka, K. Kosuge and S. Kachi, *Mater. Res. Bull.*, 1980, **15**, 521–524.
42 S. Muranaka and T. Takada, *J. Solid State Chem.*, 1975, **14**, 291–298.
43 H. Wada, *Bull. Chem. Soc. Jpn.*, 1978, **51**, 1368–1373.
44 H. Wada, *Bull. Chem. Soc. Jpn.*, 1980, **53**, 668–672.
45 I. Kawada and H. Wada, *Physica B+C*, 1981, **105**, 223–229.
46 H. Nozaki and H. Wada, *J. Solid State Chem.*, 1983, **47**, 69–80.
47 A. Powell, *J. Solid State Chem.*, 1999, **144**, 372–378.
48 A. V. Powell, D. C. Colgan and P. Vaqueiro, *J. Mater. Chem.*, 1999, **9**, 485–492.
49 T. Murugesan, S. Ramesh, J. Gopalakrishnan and C. N. R. Rao, *J. Solid State Chem.*, 1982, **44**, 119–125.
50 J. Sangster and A. D. Pelton, *J. Phase Equilib.*, 1997, **18**, 89–96.
51 E. Bekaert, P. Balaya, S. Murugavel, J. Maier and M. Ménétrier, *Chem. Mater.*, 2009, **21**, 856–861.
52 P. Balaya, A. J. Bhattacharyya, J. Jamnik, Y. F. Zhukovskii, E. A. Kotomin and J. Maier, *J. Power Sources*, 2006, **159**, 171–178.
53 L. Gireaud, S. Grugeon, S. Pilard, P. Guenot, J.-M. Tarascon and S. Laruelle, *Anal. Chem.*, 2006, **78**, 3688–3698.
54 S. Grugeon, S. Laruelle, L. Dupont and J.-M. Tarascon, *Solid State Sci.*, 2003, **5**, 895–904.
55 M. Dollé, P. Poizot, L. Dupont and J.-M. Tarascon, *Electrochem. Solid-State Lett.*, 2002, **5**, A18.
56 S. Laruelle, S. Grugeon, P. Poizot, M. Dollé, L. Dupont and J.-M. Tarascon, *J. Electrochem. Soc.*, 2002, **149**, A627.
57 R. Dedryvere, S. Laruelle, S. Grugeon, P. Poizot, D. Gonbeau and J.-M. Tarascon, *Chem. Mater.*, 2004, **16**, 1056–1061.
58 T. B. Kim, W. H. Jung, H. S. Ryu, K. W. Kim, J. H. Ahn, K. K. Cho, G. B. Cho, T. H. Nam, I. S. Ahn and H. J. Ahn, *J. Alloys Compd.*, 2008, **449**, 304–307.
59 Z. Hu, Z. Zhu, F. Cheng, K. Zhang, J. Wang, C. Chen and J. Chen, *Energy Environ. Sci.*, 2015, **8**, 1309–1316.
60 S. H. Choi and Y. C. Kang, *Nanoscale*, 2015, **7**, 6230–6237.